Boroxol Rings in Liquid and Vitreous B_2O_3 from First Principles

Guillaume Ferlat,[1] Thibault Charpentier,[2] Ari Paavo Seitsonen,[1] Akira Takada,[3] Michele Lazzeri,[1] Laurent Cormier,[1] Georges Calas,[1] and Francesco Mauri[1]

[1]*IMPMC, CNRS-IPGP-Universités Paris 6 et 7, 140, rue de Lourmel, Paris, France*
[2]*CEA, IRAMIS, Service de Chimie Moléculaire, LSDRM, F-91191 Gif-sur-Yvette, France*
[3]*Research Center, Asahi Glass Co. Ltd, 1150 Hazawa-cho, Yokohama 221-8755, Japan University College London, Gower Street, London W1E 6BT, United Kingdom*

(Received 12 March 2008; published 7 August 2008)

We investigate the structural and vibrational properties of glassy B_2O_3 using first-principles molecular dynamics simulations. In particular, we determine the boroxol rings fraction f for which there is still no consensus in the literature. Two numerical models containing either a low or a high level of boroxol rings are tested against a gamut of experimental probes (static structure factor, Raman, ^{11}B and ^{17}O NMR data). We show that only the boroxol-rich model ($f = 75\%$) can reproduce the full set of observables. Total-energy calculations show that at the glass density, boroxol-rich structures are favored by about 6 kcal/(mol boroxol). Finally, the liquid state is explored in the 2000–4000 K range and a reduction of f to 10%–20% is obtained.

DOI: 10.1103/PhysRevLett.101.065504 PACS numbers: 61.43.Fs, 61.05.−a, 61.20.Ja, 78.30.−j

Because of its importance as a prototypical glass former and as an essential component of industrial glasses, B_2O_3 has received tremendous attention [1–27]. Despite these efforts, the microscopic structure of vitreous B_2O_3 is still debated [4,5]: while it is established that the molecular building block is the planar $BO_{3/2}$ group, different models of their connectivity have been proposed from a continuous random network of corner-sharing triangles [6] to a network entirely based on hexagonal $B_3O_{9/2}$ units [7], called boroxol rings (see Fig. 1). Although there is now a broad consensus on the existence of boroxols, the debate comes as when to quantify their proportions, commonly defined by the fraction f of borons inside these rings: values on the low (~0%–30%) [8–12] or high (~60%–85%) [4,13–18] side are regularly reported.

The first experimental support for the occurrence of boroxols comes from the observation of a very sharp and highly polarized Raman peak at 808 cm^{-1} which has been attributed to the in-phase breathing mode of the oxygen atoms inside the rings (see [14] for a review). Unfortunately, the quantitative determination of the fraction of atoms involved in these rings is far from trivial due to matrix element enhancement effects in the Raman signal [28]. NMR and nuclear quadrupole resonance experiments do evidence the presence of two populations in both ^{17}O and ^{11}B spectra [16,17] which were assigned to atoms inside and outside the rings by calculations on cluster models [19] and by the comparison of the spectra with borate crystals of known structure [18]. In these studies, values of f ranging from 65% to 85% were derived from the population ratio. Little can be inferred from diffraction data analysis since f values varying from 0% to 82% have been reported. However, it has been claimed using reverse Monte Carlo simulations, that it is not possible to produce structural models containing more than 30% of boroxols that simultaneously reproduce the experimental density and the neutron and x-ray diffraction data [12].

Results in favor of boroxol-poor models have mainly been obtained from molecular dynamics (MD) simulations (e.g., [9]). Potentials including polarization or at least three-body interactions were required in order to get some boroxol rings [10,20]. The obtained f value was in any case below 30%. In these calculations, there are at least three sources of errors: the unrealistically high quench rate, the system size, and the use of empirical force fields. The first full *ab initio* MD simulation of vitreous B_2O_3 came out recently [4] and revived the discussion [5]. While the configuration obtained from the liquid quench contained only $f = 9\%$ (one boroxol for 160 atoms), strong but

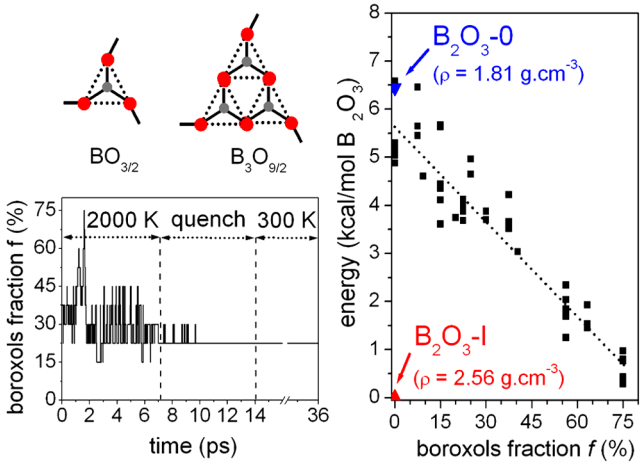

FIG. 1 (color online). Upper left: A $BO_{3/2}$ triangle and a $B_3O_{9/2}$ boroxol ring. Lower left: Evolution of the fraction of boroxols during the simulation. Right: Energy for configurations of varying boroxol amount at 0 K and $\rho = 1.84\ g \cdot cm^{-3}$.

indirect evidence was provided from Raman and ^{11}B NMR analysis that the *true* value should be ~75% (the Raman peak at 808 cm^{-1} being underestimated and the NMR population ratio being incorrect). However, this extrapolation has been immediately criticized [5]. Indeed, a model able to reproduce simultaneously all the experimental informations within a unified method has been lacking so far. Thus, as noted in the latest publications [2,3], there is yet no consensus on the f value.

In this Letter, we present the performances of boroxol-poor (BP) and boroxol-rich (BR) models regarding the above-mentioned observables (diffraction, Raman, and ^{11}B NMR data). We add in the comparison ^{17}O NMR spectra which constitute another sensitive probe of f. In addition, energetics are computed from frozen liquid snapshots.

The calculations were carried out within a first-principles approach [29] using the SIESTA code [33]. We first generated a random network of $BO_{3/2}$ triangles in a cubic box at the glass density (1.84 $g \cdot cm^{-3}$). This structure, containing 100 atoms and 4 boroxol rings ($f = 30\%$), has been used as a starting configuration for a MD simulation of the liquid at 2000 K for a duration of 20 ps using a time step of 1 fs in the NVT ensemble. After 7 ps, a quench to 300 K was branched from the previous simulation for a 7 ps duration. The system at 300 K was then sampled for 22 ps; Fig. 1. The obtained glass contains 3 boroxols ($f = 22.5\%$) and is hereafter referred to as the BP model. A shorter simulation (7 ps) was also run in the liquid at 4000 K. Average values of $\langle f \rangle \sim 13\%$ and ~17% were obtained at 4000 and 2000 K, respectively. Because of the sluggish kinetics at 2000 K, no attempt was made to sample f at lower temperature since this would be prohibitively time demanding: should the simulation time scale proportionally to the viscosity [21], an increase by a factor of 10^6 would be needed going from 2000 to 500 K. Actually, no more bond formation or breaking events were observed below ~1000 K indicating that the liquid is already supercooled on the time scale of our simulations as a result of the very high quench rate (experimentally, the glass transition temperature is $T_g = 533$ K [22]).

Thus, the f value obtained in our quenched sample is actually reflecting the liquid state around ~2000 K. This is especially annoying in the case of B_2O_3 since it is known that a drastic evolution occurs above T_g [22,23]: from monitoring Raman peak ratio, it has been derived that f decreases from ~60%–65% at 500 K to ~15%–20% at 1900 K [22], the latter value being in very good agreement with our study. However, glassy structures obtained from conventional numerical quench rates are highly likely to underestimate f given the affordable simulation times.

We thus sought for a glassy model produced by an alternative method [24] which has both $f = 75\%$ and the correct glass density [34]. This model has been used in previous MD studies [2,24] using empirical force fields, here within our first-principles scheme. MD simulations were carried out at 300 K on systems containing 80 and 320 atoms for durations of 20 and 7 ps, respectively. No size effects were observed and the structures obtained are referred to hereafter as the BR model. Liquid simulations were also carried out at 2000, 3000, and 4000 K.

In order to gain insight on the relative stability of BP and BR structures, total-energy calculations were carried out on configurations taken from the liquid trajectories and relaxed at 0 K. The zero of energies in Fig. 1 is that obtained for the B_2O_3-I crystal (stable polymorph at ambient pressure, $\rho = 2.54$ $g \cdot cm^{-3}$). Within statistical scattering, a monotonic decrease of the energy with increasing f is observed. Using a linear data fit, a slope of 6.6 ± 1 kcal/(mol boroxol) is obtained in agreement with a stabilization enthalpy of 6.4 ± 0.4 kcal/(mol boroxol) derived from Raman data [22]. We report on the same figure the energy of a hypothetical crystalline polymorph, B_2O_3-0 whose density is close to that of the glass (1.81 $g \cdot cm^{-3}$) at ambient conditions and which was recently predicted by MD simulations to be stable under tensile stress [2]; interestingly it falls well on our data at $f = 0$. Thus, at the glass density, boroxol-rich structures are more stable than boroxol-poor ones. As noted in [13], the replacement of all $BO_{3/2}$ by $B_3O_{9/2}$ units (see Fig. 1) in a given structure lowers the density; indeed, it increases the volume by a factor of 2^3 but the number of atoms only by a factor of 3. Thus, the presence of boroxols favors low-density structures [35] and explains the higher energetic stability of boroxol-rich structures at the glass densities. In this scenario, as the liquid is quenched, boroxols tend to develop to compensate the thermal densification that would otherwise occur.

To check the robustness of our calculations, we repeated on a restricted set of configurations the same relaxations using different approximations for the exchange-correlation functional, namely, local-density approximation (LDA) [36] and BLYP [37] (in addition to PBE [30]

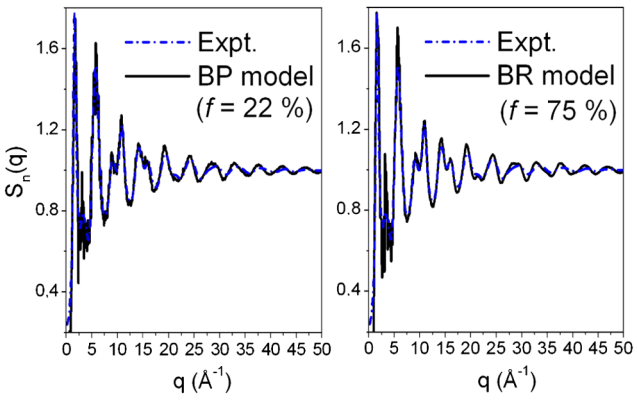

FIG. 2 (color online). Static neutron structure factor calculated for the BP and BR models (solid lines) compared with the experimental data (dash-dotted lines) [14].

used for the results shown in Fig. 1). The obtained slopes all agree with each other within ~1 kcal/(mol boroxol) [38].

We now test our BP and BR models using neutron scattering, Raman, and NMR data. The NMR chemical shifts and electric field gradients were calculated within the gauge included projector augmented wave formalism as in [39] using the PARATEC code [40]. Dynamic angle spinning (DAS) and magic angle spinning (MAS) NMR spectra of the central transition ($-\frac{1}{2} \leftrightarrow \frac{1}{2}$) were simulated taking into account both the quadrupolar and chemical shift interactions as described in [41] and including spinning sidebands. The Raman intensities were calculated as in [42] using the PWSCF code [43].

As seen in Fig. 2, both models reproduce very well [44] the experimental neutron weighted static structure factor [14], confirming that it is a poor probe of f as already mentioned [2,4]. This is in contrast with the results of [12] in which boroxol-rich models generated from reverse Monte Carlo simulations were shown to give a slightly but significantly worse agreement than boroxol-poor models as a result of some structural artifacts in the former ones (visible in the $g_{\mathrm{B\text{-}B}}(r)$ and $g_{\mathrm{B\text{-}O}}(r)$ partial distribution functions and in the O-B-O and dihedral angle distributions). We stress that none of these artifacts were observed in our BR model. We conclude that they were most probably due to the method used in [12] but are certainly not specific of BR models. The claim that it is not possible to simultaneously reproduce the diffraction data and the density for high values of f is clearly invalidated. The infrared spectra (not shown) are also in very good agreement with experiments [25] for both BP and BR models.

By contrast, the Raman spectra obtained for BP and BR models are drastically different. The main difference (Fig. 3) is in the intensity of the peak at ~800 cm^{-1} which appears in our calculations to result solely from the breathing mode of oxygens in boroxols. The area under this peak is found to be proportional to f, validating *a posteriori* the hypothesis made in [4]. While it is dramatically underestimated in the BP case, it matches the experimental one in the BR case within the error bar associated to this comparison (15%). We point out that there are no models to our knowledge in the literature which agree at this level of accuracy over such a large spectrum range. The superiority of the BR model regarding NMR spectra is also obvious (Fig. 4). For both ^{11}B and ^{17}O spectra, contributions arising from nuclei inside or outside the boroxol rings can be clearly evidenced due to the sensitivity of the NMR observables to the B-O-B angles (average values of ~120° and ~130° were obtained for in- and out-of rings triplets, respectively).

In conclusion, the comparison of BR and BP models straightforwardly identifies the observables sensitive to the boroxol fraction. The BR model is the only one able to reproduce the experimental data. Our results indicate that the liquid state is characterized by a large viscosity and small values of f. Thus, the large underestimation of f in MD models is due to the use of unrealistically fast quenching rates. Our calculations evidence an energy gain with increasing f in very good agreement with previous indirect experimental [22] and theoretical [27] determinations. This study reveals the role played by the boroxols: they allow one to maintain a low-energy structure while keeping a liquidlike density. Finally, the achievement of a realistic glassy model up to a medium-range scale opens new

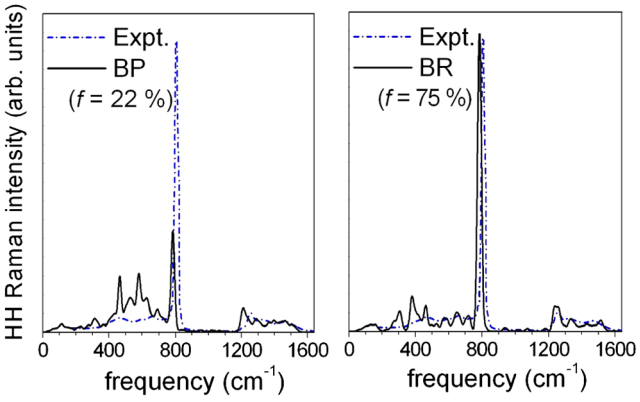

FIG. 3 (color online). Reduced horizontal-horizontal (HH) Raman spectra calculated for the BP and BR models (solid lines) compared with the experimental spectra (dash-dotted lines) [25]. A Gaussian broadening of 10 cm^{-1} is applied.

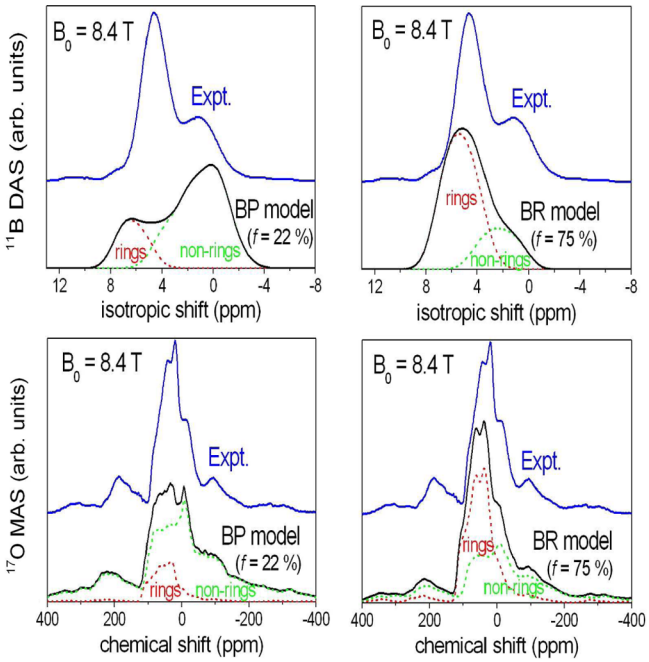

FIG. 4 (color online). ^{11}B DAS (isotropic projection) and ^{17}O MAS NMR spectra calculated for the BP and BR models compared to the experimental spectra [17]. The contributions from nuclei inside or outside the boroxol rings are also shown (dashed lines). A Gaussian broadening of 100 Hz is applied.

perspectives for high-pressure investigations of B_2O_3 and for studies of related systems such as borates or borosilicates.

Part of the calculations were carried out at the IDRIS and CCRT supercomputers.

[1] J. Nicholas, S. Sinogeikin, J. Kieffer, and J. Bass, Phys. Rev. Lett. **92**, 215701 (2004); S. K. Lee, K. Mibe, Y. Fei, G. D. Cody, and B. O. Mysen, Phys. Rev. Lett. **94**, 165507 (2005); S. K. Lee *et al.*, Nature Mater. **4**, 851 (2005); V. Brazhkin *et al.*, JETP Lett. **78**, 393 (2003); **79**, 308 (2004).

[2] L. Huang and J. Kieffer, Phys. Rev. B **74**, 224107 (2006); L. Huang, M. Durandurdu, and J. Kieffer, J. Phys. Chem. C **111**, 13712 (2007).

[3] G. Simon, B. Hehlen, R. Vacher, and E. Courtens, Phys. Rev. B **76**, 054210 (2007).

[4] P. Umari and A. Pasquarello, Phys. Rev. Lett. **95**, 137401 (2005); **96**, 199702 (2006).

[5] J. Swenson and L. Börjesson, Phys. Rev. Lett. **96**, 199701 (2006).

[6] W. H. Zachariasen, J. Am. Chem. Soc. **54**, 3841 (1932).

[7] J. Krogh-Moe, J. Non-Cryst. Solids **1**, 269 (1969).

[8] S. J. Williams and S. R. Elliott, Proc. R. Soc. A **380**, 427 (1982).

[9] T. F. Soules, J. Chem. Phys. **73**, 4032 (1980); W. Soppe, W. F. van der Marela, and H. W. den Hartog, J. Non-Cryst. Solids **101**, 101 (1988).

[10] M. Teter, in *Borate Glasses, Crystals and Melts*, edited by A. C. Wright, S. A. Feller, and A. C. Hannon (Society of Glass Technology, Sheffield, England, 1997), p. 407.

[11] E. Chason and F. Spaepen, J. Appl. Phys. **64**, 4435 (1988); K. Suzuya, Y. Yoneda, S. Kohara, and N. Umesaki, Phys. Chem. Glasses **41**, 282 (2000).

[12] J. Swenson and L. Börjesson, Phys. Rev. B **55**, 11 138 (1997).

[13] R. J. Bell and A. Carnevale, Philos. Mag. B **43**, 389 (1981).

[14] A. C. Hannon *et al.*, J. Non-Cryst. Solids **177**, 299 (1994).

[15] R. N. Sinclair *et al.*, Phys. Chem. Glasses **41**, 286 (2000).

[16] G. E. J. Jellison, L. W. Panek, P. J. Bray, and G. B. J. Rouse, J. Chem. Phys. **66**, 802 (1977); S. J. Gravina and P. J. Bray, J. Magn. Reson. **89**, 515 (1990); S.-J. Hwang *et al.*, Solid State Nucl. Magn. Reson. **8**, 109 (1997); C. Joo, U. Werner-Zwanziger, and J. W. Zwanziger, J. Non-Cryst. Solids **261**, 282 (2000); S. Kroeker, P. S. Neuhoff, and J. F. Stebbins, J. Non-Cryst. Solids **293–295**, 440 (2001).

[17] R. E. Youngman and J. W. Zwanziger, J. Non-Cryst. Solids **168**, 293 (1994); R. E. Youngman *et al.*, Science **269**, 1416 (1995).

[18] S. Kroeker and J. F. Stebbins, Inorg. Chem. **40**, 6239 (2001).

[19] J. A. Tossell, J. Non-Cryst. Solids **183**, 307 (1995); **215**, 236 (1997); J. W. Zwanziger, Solid State Nucl. Magn. Reson. **27**, 5 (2005).

[20] A. Takada, C. R. A. Catlow, and G. D. Price, J. Phys. Condens. Matter **7**, 8693 (1995); R. Fernández-Perea, F. J. Bermejo, and M. L. Senent, Phys. Rev. B **54**, 6039 (1996); J. K. Maranas, Y. Chen, D. K. Stillinger, and F. H. Stillinger, J. Chem. Phys. **115**, 6578 (2001).

[21] N. S. Srinivasan, J. M. Juneja, and S. Seetharaman, Metall. Mater. Trans. A **25**, 877 (1994).

[22] G. E. Walrafen, S. R. Samanta, and P. N. Krishnan, J. Chem. Phys. **72**, 113 (1980).

[23] A. K. Hassan, L. M. Torell, L. Börjesson, and H. Doweidar, Phys. Rev. B **45**, 12 797 (1992).

[24] A. Takada, C. R. A. Catlow, and G. D. Price, Phys. Chem. Glasses **44**, 147 (2003); A. Takada, Phys. Chem. Glasses **45**, 156 (2004).

[25] F. L. Galeener, G. Lucovsky, and J. C. Mikkelsen, Jr., Phys. Rev. B **22**, 3983 (1980).

[26] N. E. Shmidt, Russ. J. Inorg. Chem. **11**, 241 (1966).

[27] M. Micoulaut, R. Kerner, and D. M. dos Santos-Loff, J. Phys. Condens. Matter **7**, 8035 (1995).

[28] However, this mode is also visible in inelastic neutron scattering spectra [15]. The comparison with data from borate crystals of known f supports that $f > 67\%$ [15].

[29] The electronic structure is described within a generalized gradient approximation [30] to density functional theory. We used norm-conserving pseudopotentials [31], double-zeta polarized basis sets, and a 280 Ry cutoff for the real-space grid. Tests on borate crystals can be found in [32].

[30] J. P. Perdew, K. Burke, and M. Ernzerhof, Phys. Rev. Lett. **77**, 3865 (1996).

[31] N. Troullier and J. L. Martins, Phys. Rev. B **43**, 1993 (1991).

[32] G. Ferlat *et al.*, Eur. J. Glass Sci. Technol. B **47**, 441 (2006).

[33] J. M. Soler *et al.*, J. Phys. Condens. Matter **14**, 2745 (2002).

[34] This model was obtained from topological modifications of the Cs_2O-$9B_2O_3$ crystal structure so as to remove the caesium atoms and delete or create some bonds, this low-alkali compound being the closest known analogue to the putative υ-B_2O_3 structure.

[35] Evidences for a locally less dense structure in the BR case is supported by the inspection of the B-B and O-O second coordination shells, not shown here.

[36] D. M. Ceperley and B. J. Alder, Phys. Rev. Lett. **45**, 566 (1980).

[37] A. D. Becke, Phys. Rev. A **38**, 3098 (1988); C. Lee, W. Yang, and R. G. Parr, Phys. Rev. B **37**, 785 (1988).

[38] However, the obtained energy difference between the more stable glassy configuration ($f = 75\%$) and the B_2O_3-I crystal shows significative dependency upon the approximation used: from -1.5 kcal/mol for BLYP to $+10.1$ kcal/mol for LDA (the experimental enthalpy difference being $+4.4$ kcal/mol at 300 K [26]).

[39] C. J. Pickard and F. Mauri, Phys. Rev. B **63**, 245101 (2001).

[40] http://www.nersc.gov/projects/paratec/.

[41] T. Charpentier and J. Virlet, Solid State Nucl. Magn. Reson. **12**, 227 (1998).

[42] M. Lazzeri and F. Mauri, Phys. Rev. Lett. **90**, 036401 (2003).

[43] S. Baroni *et al.*, http://www.pwscf.org.

[44] For both models, a slight overstructuration and a frequency misfit are visible at high q which result from well-known tendencies of the PBE functional (B-O average bond length of 1.38 Å instead of 1.37 Å experimentally).